
Relaxed Conformal Prediction Cascades for Efficient Inference Over Many Labels

Adam Fisch* **Tal Schuster*** **Tommi Jaakkola** **Regina Barzilay**
 Computer Science and Artificial Intelligence Laboratory
 Massachusetts Institute of Technology
 {fisch,tals,tommi,regina}@csail.mit.edu

Abstract

Providing a small set of promising candidates in place of a single prediction is well-suited for many open-ended classification tasks. Conformal Prediction (CP) is a technique for creating classifiers that produce a valid set of predictions that contains the true answer with arbitrarily high probability. In practice, however, standard CP can suffer from both low *predictive* and *computational* efficiency during inference—i.e., the predicted set is both unusably large, and costly to obtain. This is particularly pervasive in the considered setting, where the correct answer is not unique and the number of total possible answers is high. In this work, we develop two simple and complementary techniques for improving both types of efficiencies. First, we relax CP validity to arbitrary criterions of success—allowing our framework to make more efficient predictions while remaining “equivalently correct.” Second, we amortize cost by conformalizing prediction cascades, in which we aggressively prune implausible labels early on by using progressively stronger classifiers—while still guaranteeing marginal coverage. We demonstrate the empirical effectiveness of our approach for multiple applications in natural language processing and computational chemistry for drug discovery.¹

1 Introduction

The ability to provide precise performance guarantees is critical to many classification tasks [1; 24; 25]. Often, however, achieving perfect accuracy may be out of reach: perhaps due to inherent noise, limited data, insufficient modeling capacity, or a host of other common pitfalls. On the other hand, in numerous applications, it can be more feasible and ultimately as useful to hedge predictions by having the classifier return a *set* of plausible options—one of which is likely to be correct.

Consider the example of large-scale, open-domain information retrieval (IR) for fact verification [54]. Here the goal is to retrieve a snippet of text of some granularity (e.g., a sentence, paragraph, or article) that can be used to support or refute a given claim. Large resources, such as Wikipedia, can contain millions of candidate snippets—many of which may independently be able to serve as viable evidence. After the retrieval stage, all flagged contexts must be reviewed in a follow-up step (perhaps even by a human) in order to yield a final verdict. A good evidence retriever should make precise snippet suggestions, quickly—but do so without excessively sacrificing sensitivity (i.e., recall).

Conformal prediction (CP) [19; 59] is a methodology for placing exactly that sort of prediction bet. Concretely, suppose we have been given n examples, $(X_i, Y_i) \in \mathcal{X} \times \mathcal{Y}$, $i = 1, \dots, n$, as training data, that have been drawn exchangeably from an underlying distribution P . For instance, in our IR setting, X would be the claim in question, Y a viable piece of evidence that supports or refutes it, and \mathcal{Y} a large corpus (e.g., Wikipedia). Next let X_{n+1} be a new exchangeable test example (e.g., a

*Equal contribution (order decided randomly).

¹Our code is available at <https://github.com/ajfisch/conformal-cascades>.

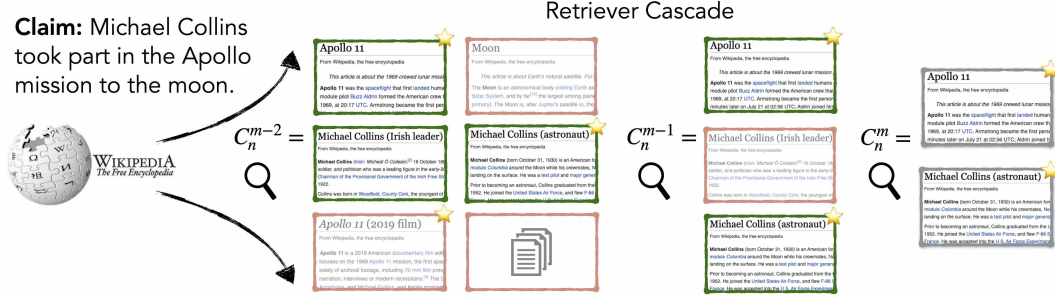


Figure 1: A demonstration of our conformalized cascade for m -step inference with set-valued outputs, here on an IR for claim verification task. The number of considered documents is reduced at every level—red frames are filtered, while green frames pass on. We only care about retrieving *at least one* of the “equivalently correct” documents (starred) that can be used to resolve the claim.

new claim to verify) for which we would like to predict the paired $y \in \mathcal{Y}$. The aim of conformal prediction is to construct a set of candidates $\mathcal{C}_{n,\epsilon}(X_{n+1})$ likely to contain Y_{n+1} (e.g., the relevant evidence) with *distribution-free marginal coverage* at an arbitrary significance level ϵ :

$$\mathbb{P}(Y_{n+1} \in \mathcal{C}_{n,\epsilon}(X_{n+1})) \geq 1 - \epsilon; \quad \text{for all distributions } P. \quad (1)$$

The marginal coverage guarantee above is jointly over X and Y , i.e., taken over all the train-test permutations of $\{(X_i, Y_i)\}_{i=1}^{n+1}$. A classifier is considered to be *valid* if the frequency of error, $Y_{n+1} \notin \mathcal{C}_{n,\epsilon}(X_{n+1})$, does not exceed ϵ . In our IR setting, this would mean including the correct document at least ϵ fraction of the time. Not all valid classifiers, however, are particularly useful (e.g., a trivial classifier that merely returns all possible outputs). A classifier is considered to have *good predictive efficiency* if $\mathbb{E}[|\mathcal{C}_{n,\epsilon}(X_{n+1})|]$ is small (i.e., $\ll |\mathcal{Y}|$). In our IR setting, this would mean not returning too many irrelevant documents. In practice, in domains where the number of outputs to choose from is large and the “correct” one is not necessarily unique, classifiers derived using conformal prediction can suffer dramatically from both poor predictive and computational efficiency [6; 61; 62]. Unfortunately, these two conditions tend to be compounding: large label spaces \mathcal{Y} both (1) often place strict constraints on the set of tractable model classes available for consideration, and (2) frequently contain multiple clusters of labels that are difficult to discriminate between, especially for a low-capacity classifier [5; 26; 36].

In this paper, we present two simple yet effective extensions for improving the efficiency of conformal prediction for open-ended problems with large output spaces \mathcal{Y} , in which several $y \in \mathcal{Y}$ might be “good enough.” First, in Section 4 we describe a generalization of Eq. 1 for marginal coverage over equivalence classes, where we ensure that at least one “equivalently correct” y is in $\mathcal{C}_{n,\epsilon}(X_{n+1})$ with high probability. For example, in our IR setting, given the claim “*Michael Collins took part in the Apollo mission to the moon*,” any of the candidate Wikipedia articles such as *Apollo 11*, *Michael Collins (astronaut)*, or *Apollo 11 (2019 film)* have enough information to independently support it (see Figure 1). When Y_{n+1} is not unique, forcing the classifier to hedge for the worst case—in which a specific realization of Y_{n+1} must be contained in $\mathcal{C}_{n,\epsilon}(X_{n+1})$ —is too strict and can lead to conservative predictions. We both suggest theoretically and show empirically that optimizing instead for our relaxed condition yields classifiers with significantly better predictive efficiency.

Second, in Section 5 we present a technique for conformalizing *prediction cascades* to progressively filter the number of candidates with a sequence of increasingly complex classifiers. This allows us to balance predictive efficiency with computational efficiency during inference. Importantly, we theoretically show that—in contrast to other similarly motivated pipelines—our method filters the output space in a manner that still guarantees marginal coverage. Figure 1 illustrates our combined approach. We demonstrate that, together, these two simple extensions serve as complementary pieces of the puzzle towards making CP more efficient. We empirically validate our approach on information retrieval for fact verification, extractive question answering, and in-silico screening for drug discovery.

Contributions. In summary, our main results are as follows:

- A theoretical relaxation of validity (Eq. 1) to account for *equivalently correct* answers.
- A principled framework for conformalizing computationally efficient prediction cascades.

- Consistent empirical gains on three diverse tasks demonstrating up to $2.7\times$ better efficiency AUC (across all ϵ) when calibrating for equivalent correctness with conformalized prediction cascades, and computation pruning rates of up to 64%—while still maintaining validity.

2 Related work

Confident prediction. Methods for obtaining precise uncertainty estimates, especially in the context of classification, have received intense interest in recent years. A significant body of work is concerned with *calibrating* model confidence—measured as $\max p_\theta(y_{n+1}|x_{n+1})$ —such that the true error rate, $y_{n+1} = \hat{y}_{n+1}$ where $\hat{y}_{n+1} = \operatorname{argmax} p_\theta(y_{n+1}|x_{n+1})$, is indeed equal to the estimated probability [18; 28; 31; 37]. In theory, these estimates could be leveraged to create confident prediction sets $\mathcal{C}_{n,\epsilon}(X_{n+1})$. Unlike CP, however, these methods are not guaranteed to be accurate, and often still suffer from miscalibration in practice—especially for modern neural networks [2; 21; 22]. *Selective classification* [14; 20], where models have the option to abstain from answering when not confident, is similar in motivation to Eq. 1. In fact, it can be considered a sub-case of CP in which the classifier chooses to abstain unless $|\mathcal{C}_{n,\epsilon}(X_{n+1})| = 1$.

Conformal prediction. As validity is already guaranteed by design, most efforts in CP focus on improving various aspects of efficiency. Mondrian CP [59] accounts for the fact that some classes are harder to model than others, and leverages class-conditional statistics. Similarly, recent work by Cauchois et al. [7] builds towards conditional—as opposed to marginal—coverage by conformalizing quantile functions [see also 44; 45] that vary with x , and also by modeling dependencies among y variables. Our method for *equivalent correctness*, on the other hand, aggregates statistics by example and across classes. Inductive CP [39] is a complementary extension that dramatically reduces the cost of computing $\mathcal{C}_{n,\epsilon}(X_{n+1})$ in the general case; we also make use of it here. Most similar to our work, trimmed [10] and discretized [11] CP trade *predictive* efficiency for *computational* efficiency in regression tasks, where the label space is infinite. A key distinction of our procedure is that we do not force the same trade-off: in fact, we empirically show that our conformalized cascades can at times result in *increased* predictive efficiency alongside a pruned label space.

Prediction cascades. The idea of balancing inference cost with accuracy using multi-step inference has been explored extensively for many machine learning applications [8; 17; 27; 33; 46]. Some of these are heuristic (i.e., with no performance guarantees), such as greedy pipelines where the top (fixed) k predictions are passed on to the next level [9; 16]. Closer to our work, Weiss and Taskar [63] optimize their cascades for overall pruning efficiency, and not for top-1 prediction. While they also analyze error bounds for filtering, their guarantees are specific to linear classifiers with bounded L_2 norm, whereas our conformalized approach only assumes data exchangeability. Furthermore, they assume a target filtering loss before training—our significance level ϵ is defined at test time.

3 Background

We begin with a brief review of conformal prediction for classification [see also 39; 51; 59; 60]. Here, and in the rest of the paper, upper-cased letters (e.g., X) denote random variables; lower-cased letters (e.g., x) denote constants, and script letters (e.g., \mathcal{X}) denote sets, unless otherwise specified.

3.1 Conformal hypothesis testing

At the core of conformal prediction is a simple statistical hypothesis test: for each candidate $y \in \mathcal{Y}$ we must either accept or reject the null hypothesis that the example $(X_{n+1} = x_{n+1}, Y_{n+1} = y)$ is a correct pairing. Formally, we rely on a *nonconformity measure* $\mathcal{S}((x_{n+1}, y), \mathcal{D})$ to serve as the test statistic, where \mathcal{S} reflects the degree to which (x_{n+1}, y) “conforms” to the distribution specified by dataset \mathcal{D} . For instance, \mathcal{S} could be computed as $-\log p_\theta(y|x)$, where θ is a model fit to \mathcal{D} .

Definition 1 (Nonconformity measure). Let $Z := \mathcal{X} \times \mathcal{Y}$ be the space of examples (X, Y) , and let $Z^{(*)} := \bigcup_{d \geq 1} (\mathcal{X} \times \mathcal{Y})^d$ be the space of datasets of examples \mathcal{D} , of any size $d \geq 1$. A *nonconformity measure* \mathcal{S} is then a measurable mapping $\mathcal{S}: Z \times Z^{(*)} \rightarrow \mathbb{R}$, that assigns a real-valued score to any example (X, Y) , indicating how “different”² it is from a reference dataset \mathcal{D} .

To be specific, exact or *full* CP takes \mathcal{D} to be all of the examples seen so far, including the candidate (x_{n+1}, y) . Thus, the nonconformity measure \mathcal{S} has to be re-trained each time. An alternative—which

²The definition of “different” here is intentionally vague, as any metric will technically work (see [59]).

we use in this paper *w.l.o.g.*—is the inductive or *split* CP variant [39] which assumes that \mathcal{D} is a proper training set, independent of any of the subsequent $n + 1$ exchangeable examples being used for CP. Dropping \mathcal{D} for ease of notation, we denote the nonconformity score for example $(X = x, Y = y)$ as $V^{(x,y)} := \mathcal{S}(X, Y)$. The degree of nonconformity can then be quantified using a p-value (Eq. 2).

3.2 Conformal prediction

To construct the final conformal *prediction*, the classifier uses the p-values to include all y for which the null hypothesis—i.e., that the candidate pair (x_{n+1}, y) is *conformal*—is not rejected.

Lemma 1 (Smoothed empirical p-value). *Assume that the random variables V_1, \dots, V_{n+1} are exchangeable. We define the smoothed empirical p-value $\text{pvalue}(V_{n+1}, V_{1:n})$ as*

$$\text{pvalue}(V_{n+1}, V_{1:n}) := \frac{|\{i \in [1, n] : V_i > V_{n+1}\}| + \tau \cdot |\{i \in [1, n] : V_i = V_{n+1}\}| + 1}{n+1}, \quad (2)$$

where $\tau \sim U(0, 1)$. Then, for any $\epsilon \in (0, 1)$, we have $\mathbb{P}(\text{pvalue}(V_{n+1}, V_{1:n}) \leq \epsilon) \leq \epsilon$.

Theorem 1 (Vovk et al. [59]; see also [32; 55]). *Assume that the random variables $(X_i, Y_i) \in \mathcal{X} \times \mathcal{Y}$, $i = 1, \dots, n + 1$ are exchangeable. For any nonconformity measure \mathcal{S} , and significance level $\epsilon \in (0, 1)$, define the conformal label set (based on the first n samples) at $x_{n+1} \in \mathcal{X}$ as*

$$\mathcal{C}_{n,\epsilon}(x_{n+1}) := \left\{ y \in \mathcal{Y} : \text{pvalue} \left(V_{n+1}^{(x_{n+1}, y)}, V_{1:n}^{(x_{1:n}, y_{1:n})} \right) > \epsilon \right\}, \quad (3)$$

where pvalue and $V_i^{(x_i, y_i)}$ are as defined previously. Then $\mathcal{C}_{n,\epsilon}(X_{n+1})$ satisfies Eq. 1.

4 Relaxed conformal prediction coverage

We introduce our first strategy for improving the *predictive efficiency* of CP classifiers, particularly when the value Y_{n+1} must take to be considered “good enough” is not well-defined. We show that it can be preferable to define a *success criterion*, rather than check for strict equality with Y_{n+1} .

4.1 Equivalent correctness and equivalent coverage

What might it mean for y to be “good enough?” Among other factors, this depends on the task, the structure of the label space \mathcal{Y} , and even the input x . For example, in IR, two different texts might both independently provide the necessary and sufficient information for claim x to be resolved. Let $R(x)$ be an equivalence relation over \mathcal{Y} , where for a given x and y we have the equivalence class:

$$[y]_{R(x)} := \{\tilde{y} \in \mathcal{Y} : \tilde{y} R(x) y\}. \quad (4)$$

In practice, we may take $\tilde{y} R(x) y$ if for some choice of comparator g and threshold c , we have $g(\tilde{y}, y, x) \geq c$. Any prediction that is a member of the equivalence class derived from this metric is considered to be *equivalently correct*, i.e., a success. For example, in IR for claim verification, this might be defined as any context \tilde{y} for which a fixed “judge” model f that decides the final verdict obeys $|f(y, x) - f(\tilde{y}, x)|^{-1} \geq c$. This leads us to a helpful definition of equivalent coverage.

Definition 2 (Equivalent marginal coverage). *Given any equivalence relation $R(X)$ over \mathcal{Y} and data points $\{(X_i, Y_i)\}_{i=1}^n$ drawn exchangeably from an underlying distribution P , a conformal predictor producing outputs $\mathcal{C}_{n,\epsilon}(X_{n+1})$ (based on the first n points) for a new exchangeable test example X_{n+1} is considered to have *equivalent marginal coverage* if for any $\epsilon \in (0, 1)$, $\mathcal{C}_{n,\epsilon}$ satisfies*

$$\mathbb{P} \left(|[Y_{n+1}]_{R(X_{n+1})} \cap \mathcal{C}_{n,\epsilon}(X_{n+1})| \geq 1 - \epsilon \right) \geq 1 - \epsilon; \quad \text{for all distributions } P; \quad (5)$$

where $[Y]_{R(X)}$ is a random variable over sets with the value $[y]_{R(x)}$ when $Y = y$ and $X = x$.

4.2 Calibrating for equivalent coverage

The introduction of the more general coverage criterion expressed in Eq. 5—as opposed to strict set membership—changes the objective. The label Y_{n+1} is no longer unique; we need only to identify at least one that is deemed equivalent according to $R(X_{n+1})$. As such, we propose a modification that allows the classifier to be more discriminative when testing the null hypothesis that y is not just conforming, but that it is the *most conforming* equivalently correct \tilde{y} for x . For each data point $(X_i = x_i, Y_i = y_i)$, we then define the minimal nonconformity score as

$$M_i^{(x_i, y_i)} := \min \left\{ V_i^{(x_i, \tilde{y})} : \tilde{y} \in [y_i]_{R(x_i)} \right\}, \quad (6)$$

and use these random variables to compute the p-values for our conformal predictor.

Theorem 2. Assume that $(X_i, Y_i) \in \mathcal{X} \times \mathcal{Y}$, $i = 1, \dots, n+1$ are exchangeable. For any nonconformity measure \mathcal{S} , equivalence relation $R(X)$ on \mathcal{Y} , and significance level $\epsilon \in (0, 1)$, define the conformal set (based on the first n samples) at $x_{n+1} \in \mathcal{X}$ as

$$\mathcal{C}_{n,\epsilon}^{\min}(x_{n+1}) := \left\{ y \in \mathcal{Y} : \text{pvalue}\left(V_{n+1}^{(x_{n+1}, y)}, M_{1:n}^{(x_{1:n}, y_{1:n})}\right) > \epsilon \right\}, \quad (7)$$

where pvalue , $V_i^{(x_i, y_i)}$, and $M_j^{(x_j, y_j)}$ are as defined previously. Then $\mathcal{C}_{n,\epsilon}^{\min}$ satisfies Eq. 5. Furthermore, we have $\mathbb{E}[|\mathcal{C}_{n,\epsilon}^{\min}(X_{n+1})|] \leq \mathbb{E}[|\mathcal{C}_{n,\epsilon}(X_{n+1})|]$, where $\mathcal{C}_{n,\epsilon}(X_{n+1})$ is as defined in Eq. 3.

Remark. Without randomization in pvalue , we get the result of $\mathcal{C}_{n,\epsilon}^{\min}(X_{n+1}) \subseteq \mathcal{C}_{n,\epsilon}(X_{n+1})$.

We present a proof in Appendix A.3. An important result of Theorem 2 is that we can guarantee better or equal predictive efficiency than standard CP, while still maintaining equivalent coverage. In Section 7 we demonstrate empirically that this simple modification can yield large improvements.

5 Conformal prediction cascades

We introduce our second strategy for improving the *computational efficiency* of conformal prediction classifiers. As is apparent from Eq. 3, the cost of conformal prediction is linear in $|\mathcal{Y}|$. In practice, this can limit the tractable choices available for the nonconformity measure \mathcal{S} , particularly in domains where $|\mathcal{Y}|$ is large. Computational efficiency can therefore directly limit predictive efficiency: the predictive efficiency of the classifier is predicated by the statistical power, $\mathbb{P}\{\text{reject } y \mid y \text{ is incorrect}\}$, of the underlying hypothesis test—which, in turn, is determined by \mathcal{S} .

Our approach balances the two by leveraging prediction cascades [17; 48; 63, *inter alia*], where m models of increasing power (and decreasing computational efficiency) are applied sequentially. We perform multi-step inference, in which the number of considered outputs is iteratively pruned. Critically, we *conformalize* the cascade (Theorem 3), which allows us to retain marginal coverage.

5.1 Pruning the label space with prediction cascades

When constructing $\mathcal{C}_{n,\epsilon}(X_{n+1})$, a nonconformity score is computed for every candidate $y \in \mathcal{Y}$. The sensitivity necessary for good predictive efficiency, however, depends on X_{n+1} , as different examples may be easier or harder than others. Imagine that we are given a sequence of progressively more discriminative, yet also more expensive, nonconformity measures $(\mathcal{S}_1, \dots, \mathcal{S}_m)$. When applied sequentially, we only consider $y \in \mathcal{C}_{n,\epsilon}^i(X_{n+1})$ as candidates for inclusion in $\mathcal{C}_{n,\epsilon}^{i+1}(X_{n+1})$. Thus,

$$\mathcal{C}_{n,\epsilon}^m(X_{n+1}) \subseteq \mathcal{C}_{n,\epsilon}^{m-1}(X_{n+1}) \subseteq \dots \subseteq \mathcal{C}_{n,\epsilon}^1(X_{n+1}) \subseteq \mathcal{Y}. \quad (8)$$

The operating assumption here is that the amortized total cost of evaluating a subset of the m measures over *parts* of \mathcal{Y} can be lower than the cost of running one expensive measure over *all* of it. When not applied as a cascade, this becomes equivalent to combined conformal prediction, where multiple conformal measures are computed in parallel and then aggregated [12; 34; 56; 57]. Combining multiple nonconformity measures can potentially lead to better and more robust predictive efficiency when using complementary measures—similar in theory to ensembles or mixtures-of-experts [23].

5.2 Maintaining distribution-free marginal coverage

Naïvely applying multiple hypothesis tests to the same data, one for each level of the cascade, leads to the well-known *multiple hypothesis testing* (MHT) problem (see Appendix D for background). This will result in an increased *family-wise error rate* (i.e., false positives), and makes the CP invalid.³ Many corrective procedures exist in the literature (e.g., see [15; 35] for a review). Formally, given m p-values $(P_1^{(x,y)}, \dots, P_m^{(x,y)})$ for a pair (x, y) , we denote as \mathcal{M} some such correction satisfying

$$\tilde{P}^{(x,y)} = \mathcal{M}\left(P_1^{(x,y)}, \dots, P_m^{(x,y)}\right) \text{ s.t. } \mathbb{P}\left(\tilde{P}^{(x,y)} \leq \epsilon \mid y \text{ is correct}\right) \leq \epsilon. \quad (9)$$

Furthermore, we require \mathcal{M} to be element-wise monotonic,⁴ i.e. (where \preccurlyeq operates element-wise):

$$\left(P_1^{(x,y)}, \dots, P_m^{(x,y)}\right) \preccurlyeq \left(\hat{P}_1^{(x,y)}, \dots, \hat{P}_m^{(x,y)}\right) \Rightarrow \mathcal{M}\left(P_1^{(x,y)}, \dots, P_m^{(x,y)}\right) \leq \mathcal{M}\left(\hat{P}_1^{(x,y)}, \dots, \hat{P}_m^{(x,y)}\right). \quad (10)$$

³Consider flipping a biased coin n times with ϵ -probability of heads, and rejecting y if at any toss is heads. As $n \rightarrow \infty$ this event will happen infinitely often for any $\epsilon > 0$, and y will always be trivially rejected.

⁴Note that we are unaware of any common \mathcal{M} beyond contrived examples satisfying (9) but not (10).

Algorithm 1 Cascaded inductive conformal prediction with distribution-free marginal coverage.

Definitions $(\mathcal{S}_1, \dots, \mathcal{S}_m)$ is a sequence of nonconformity measures. \mathcal{M} is a monotonic correction controlling for family-wise error. $x_{n+1} \in \mathcal{X}$ is the given test point. $x_{1:n} \in \mathcal{X}^n$ and $y_{1:n} \in \mathcal{Y}^n$ are the previously observed conformal training examples and their labels, respectively. \mathcal{Y} is the label space. ϵ is the significance.

```

1: function PREDICT( $x_{n+1}, (x_{1:n}, y_{1:n}), \epsilon$ )
2:    $\mathcal{C}_{n,\epsilon}^0 \leftarrow \mathcal{Y}$                                  $\triangleright$  Initialize with the full label set.
3:    $p_1^{(y)} = p_2^{(y)} = \dots = p_m^{(y)} \leftarrow 1, \forall y \in \mathcal{Y}$      $\triangleright$  Conservatively set unknown p-values.
4:   for  $j = 1$  to  $m$  do
5:      $\mathcal{C}_{n,\epsilon}^j \leftarrow \{\}$                                  $\triangleright$  Initialize the current output.
6:     for  $y \in \mathcal{C}_{n,\epsilon}^{j-1}$  do
7:        $p_j^{(y)} \leftarrow \text{pvalue}(\mathcal{S}_j(x_{n+1}, y), S_j(x_{1:n}, y_{1:n}))$      $\triangleright$  Update the  $j$ -th p-value for  $(x_{n+1}, y)$ .
8:        $\tilde{p}_j^{(y)} \leftarrow \mathcal{M}(p_1^{(y)}, \dots, p_m^{(y)})$                        $\triangleright$  Correct the current p-values for MHT.
9:       if  $(\tilde{p}_j^{(y)} > \epsilon)$  then                                 $\triangleright$  Keep  $y$  iff the corrected p-value supports it.
10:       $\mathcal{C}_{n,\epsilon}^j \leftarrow \mathcal{C}_{n,\epsilon}^j \cup \{y\}$ 
11:   return  $\mathcal{C}_{n,\epsilon}^m$                                  $\triangleright$  Return the final output of the cascade.

```

We consider several common options for \mathcal{M} , namely the Bonferroni, Simes, and ECDF corrections. See Appendix D for technical details, and a comparison of the different methods.

How do we correct for MHT when we must decide on the outcome of the test early at cascade j , before all the p-values (i.e., those that have not yet been computed for measures $k > j$) are known? We compute an upper bound for the corrected p-value by conservatively assuming that $P_k^{(x,y)} = 1$, $\forall k > j$. The full procedure is demonstrated in Algorithm 1, and formalized below in Theorem 3.

Theorem 3. *Assume that $(X_i, Y_i) \in \mathcal{X} \times \mathcal{Y}$, $i = 1, \dots, n+1$ are exchangeable. For any sequence of nonconformity measures $(\mathcal{S}_1, \dots, \mathcal{S}_m)$ generating p-values $(P_1^{(x_i, y_i)}, \dots, P_m^{(x_i, y_i)})$, and significance level $\epsilon \in (0, 1)$, define the conformal set for step j (based on the first n samples) at $x_{n+1} \in \mathcal{X}$ as*

$$\mathcal{C}_{n,\epsilon}^j(x_{n+1}) := \left\{ y \in \mathcal{Y} : \tilde{P}_j^{(x_{n+1}, y)} > \epsilon \right\}, \quad (11)$$

where $\tilde{P}_j^{(x_{n+1}, y)}$ is the conservative p-value for step j , $\mathcal{M}(P_1^{(x_{n+1}, y)}, \dots, P_j^{(x_{n+1}, y)}, 1, \dots, 1)$, with $P_{k>j}^{(x_{n+1}, y)} := 1$. Then $\forall j \in [1, m]$, $\mathcal{C}_{n,\epsilon}^j(X_{n+1})$ satisfies Eq. 1, and $\mathcal{C}_{n,\epsilon}^m(X_{n+1}) \subseteq \mathcal{C}_{n,\epsilon}^j(X_{n+1})$.

We present a straightforward proof in Appendix A.4, which also extends to the setting of Eq. 5. An important result of Theorem 3 is that it shows that pruning early using Algorithm 1 will not affect the final result $\mathcal{C}_{n,\epsilon}^m$, either in terms of validity or in terms of final set membership (i.e., Eq. 8 is naturally upheld). Furthermore, each level of the cascade is guaranteed to be valid, meaning that we can exit the entire prediction process early at any time (e.g., as soon as $|\mathcal{C}_{n,\epsilon}^j|$ is below some desired threshold). In Section 7 we demonstrate empirically that, for many applications, even simple choices for $\mathcal{S}_{j < m}$ can allow for a substantial number of candidates to be pruned early (i.e., before step m).

6 Experimental setup

We empirically evaluate our method on three different tasks with standard, publicly available datasets. In this section, we briefly outline each task and our motivations for including it. We also describe our evaluation methodology. Additional technical details for each task are included in Appendix C.

6.1 Tasks

Extractive question answering (QA). Given a question q and a supporting context c with l tokens, (c_1, \dots, c_l) , extractive QA finds a span $[i, j] \subseteq [1, l]$ that can be used to answer q . We use the SQuAD 2.0 dataset [41], which also contains unanswerable questions, modeled here with an explicit “no answer” option. There are many possible answer spans ($\mathcal{O}(l^2) + 1$) and they are non-unique. A span that matches any of the labelled answers (typically 1-3) when lower-cased and stripped of articles and punctuation is considered to be equivalently correct. Our cascade consists of (1) scores from an ALBERT [29] model that predicts span start and end points i, j independently (\sim linear run-time), and (2) scores from an ALBERT model that predicts i and j jointly (\sim quadratic run-time).

Information retrieval for fact verification (IR). As introduced in §1, the goal of IR for fact verification is to retrieve a sentence that can be used to support or refute a given claim. We use claims from the FEVER dataset [54], in which evidence is sourced from a set of $\sim 40K$ sentences collected from Wikipedia. Any sentence that provides enough evidence to enable a verdict is considered to be equivalently correct (multiple are labelled). Our cascade consists of (1) a quick, non-neural BM25 similarity score (following Řehůřek and Sojka [42]) between a given claim and sentence, and (2) the score of an ALBERT model trained to directly predict if a given claim and sentence are related.

In-silico screening for drug discovery (DR). In-silico screening of chemical compounds is a common task in drug discovery/repurposing, where the goal is to identify possibly effective drugs to manufacture and test [53]. We simulate this task using a dataset of 41,127 molecules screened for HIV inhibition [65]. The dataset contains 1,443 positives. We partition the dataset into multiple “screens,” where for each screen 100 total candidates are randomly sampled (the positives are not replaced and are disjoint between screens). Our cascade consists of (1) metrics derived from a Random Forest (RF) applied to binary Morgan fingerprints [43], and (2) the score of an ensemble of five Directed Message Passing Neural Networks (implemented with *chemprop* [66]). Note that the inference time of the RF (on CPU) is $\sim 50\times$ faster than *chemprop* with a single GPU ($\sim 10\times$ if using five GPUs).

6.2 Evaluation metrics

For each task, we use a proper training set, a validation set, and a test set. We use the training set to learn all nonconformity measures \mathcal{S} . We then perform model selection specifically for CP on the validation set, and report final numbers on the test set. For all CP evaluations (on either validation or test data), we report the marginalized results over multiple random trials (50 for QA/IR; 1K for DR), where in each trial we partition the data into 80% calibration points (the $x_{1:n}$) and 20% prediction points (the x_{n+1}). In order to compare the performance of different CPs across significance levels, we plot each metric as a function of ϵ , and compute the area under the curve (AUC). In all plots, shaded regions show the 16-84th percentiles across trials. We report the following average metrics:

Equivalent success rate. We measure the equivalent success rate as the rate at which at least one equivalently correct prediction is in $\mathcal{C}_{n,\epsilon}$, i.e., $|[Y_{n+1}]_{R(X_{n+1})} \cap \mathcal{C}_{n,\epsilon}(X_{n+1})| \geq 1$ (see Eq. 5). To be valid—the key criteria in this work—a classifier should have a success rate $\geq 1 - \epsilon$, and AUC ≥ 0.5 . Note that *more* is *not necessarily better*: higher success rates than required can lead to poor efficiency (i.e., the size of $\mathcal{C}_{n,\epsilon}$ can afford to decrease at the expense of accuracy).

Predictive efficiency (↓). We measure predictive efficiency as the size of the prediction set out of all candidates: $|\mathcal{C}_{n,\epsilon}| \cdot |\mathcal{Y}|^{-1}$. The goal is to make the predictions more precise (i.e., make $\mathcal{C}_{n,\epsilon}$ smaller) while still maintaining validity. Note that *lower* point-wise predictive efficiency and *lower* AUC is better, as it means that the size of $\mathcal{C}_{n,\epsilon}$ is relatively *smaller*.

Amortized computation cost (↓). We measure the amortized computation cost as the ratio of pvalue computations required to make a cascaded prediction with early pruning, compared to the number when using a simple combination of CPs (no pruning, same number of measures). In this work we do not measure concrete wall-clock times as these are hardware-specific, and depend heavily on the optimized implementation (e.g., batching, custom kernels, *etc*). We leave this as a follow-up. Note that *lower* point-wise amortized cost and *lower* AUC is better, as it means that the total number of pvalue computations required to construct $\mathcal{C}_{n,\epsilon}^m$ (for a given m) is relatively *smaller*.

7 Experimental results

In the following, we address several key research questions relating to our combined extensions to the conformal prediction framework, and their impact on the overall performance. In all of the following experiments we report results on the test set, using cascade configurations selected based on the validation set performance. Additional results and analysis are included in Appendix B. QA and DR experiments use the Simes correction, while IR uses the ECDF correction for MHT.

Relaxed CP and predictive efficiency. We begin by focusing on testing our method for deliberately calibrating for *equivalent* coverage rather than standard coverage (i.e., defining $\mathcal{C}_{n,\epsilon}$ by Eq. 7 vs. Eq. 3). Figure 2 shows the equivalent success rate and predictive efficiency of our relaxed *min*-cascaded CP, both compared to a cascaded CP with standard calibration and to a standard CP (using only the final metric of the cascade: CLS logit or *chemprop*). First, we observe that our relaxed version still creates valid predictors, with a success rate close to $1 - \epsilon$ on average. As expected, the

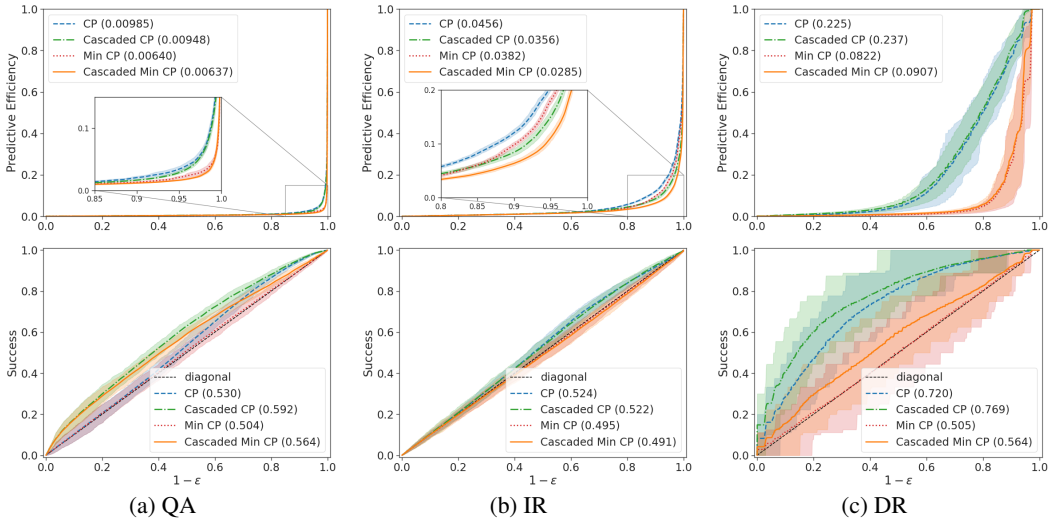


Figure 2: *Does calibrating using minimal nonconformity (§4.2) improve predictive efficiency?* We show predictive efficiency and equivalent success rates across values of epsilon. The efficiency of the *min*-calibrated cascaded CP is better (lower) than standard CP across all tasks. The *min*-calibrated CP’s success rate hugs the diagonal, allowing it to remain valid, but be far less conservative than the baseline (resulting in better efficiency). We also show the isolated effect of the cascade: in QA and IR it improves the efficiency while in DR it does not, possibly due to the small gains of chemprop over RF here. The top plots focus in areas of greatest difference (but the AUC is measured over all ϵ).

effectiveness of the CP depends on the number of points n used to calibrate $\mathcal{C}_{n,\epsilon}$. The DR task, being a dataset with few positive examples for calibration, exhibits high variance in the success rate for $\mathcal{C}_{n,\epsilon}$ (though on average, it is still valid) and becomes conservative at the tail ends (i.e., when ϵ is close to 0).⁵ This is slightly more pronounced in the cascaded versions, as the MHT correction exacerbates small sample sizes. Both IR and QA, having larger calibration sets, are largely unaffected by this and exhibit relatively lower variance. Second, we see that the *min*-calibration allows the predictor to reject more wrong predictions (lower predictive efficiency) while, with high enough probability, still accepting at least one that is correct. This effect is most pronounced at smaller ϵ (e.g., < 0.2).

Cascaded CP and computational efficiency. Next, we examine the pruning effectiveness of our cascaded approach. Figure 3 shows the amortized cost, in terms of p-value computations saved, achieved using the early rejection of our cascaded CP. Our method reduces the number of p-value computations for all candidates by 63% for a three-layer cascade (QA) and by 39%-42% for two-layer cascades (IR and DR). The effect of conformalization is clear: the more strict an ϵ we demand, the fewer labels we can prune, and vice versa. To simplify the comparisons, our metric gives equal weight to all p-value computation. Note that in practice, however, the benefit of early rejection will grow by layer, as the later nonconformity scores are assumed to be increasingly expensive to compute. Again, exactly quantifying this trade-off in terms of absolute cost is model- and implementation-specific; we leave it for future work.

Cascaded CP and predictive efficiency. Our cascaded pipeline allows for the combination of multiple measures, some of which are computationally expensive. Figure 4 shows the contribution of each layer to the final efficiency. For example, in the IR task, the BM25 CP already drastically trims the set of candidates by 90%, on average. The stronger neural classifier is then only needed on a fraction of the candidate space—and can be used to further reject more than 2/3rds of the remaining predictions, all while still preserving equivalent coverage. Note that, at times, the full cascade can remarkably lead to an ultimately more powerful predictor than even just using the strongest individual measure over all labels (which is also computationally inefficient)—see IR in Figure 2 for a positive example. This depends, however, in how complementary the nonconformity measures are. In DR, *chemprop* does provide much performance gains over RF on our tested data. Therefore, and due to some disagreements between the models and the effect of the MHT correction, the cascade increases the predictive efficiency. In QA, even though the CLS logit alone provides a strong classifier by itself (though computationally expensive), the cascade can improve slightly further.

⁵E.g., when computed over $n + 1$ values, $\text{pvalue}(\cdot, \cdot) > \epsilon \forall \epsilon < \frac{1}{n+1}$, and $\mathcal{C}_{n,\epsilon}(X_{n+1})$ degenerates to \mathcal{Y} .

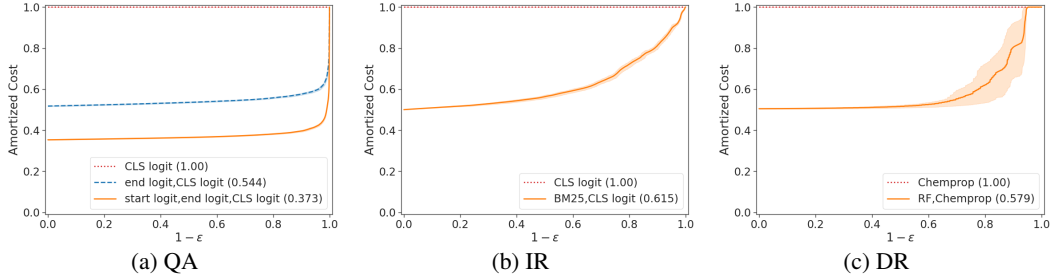


Figure 3: *How effective is cascaded conformal prediction (§5.1) at pruning the candidate space?* In a CP with no early rejection (e.g., red dotted line) we have to compute p-values for all nonconformity scores, for every candidate. Incorporating early rejection via the CP cascade reduces the total number of computations necessary—down to a factor of $1/m$, where m is the number of cascade levels. Note that even though we prune candidates early, we still maintain validity (see Figure 2).

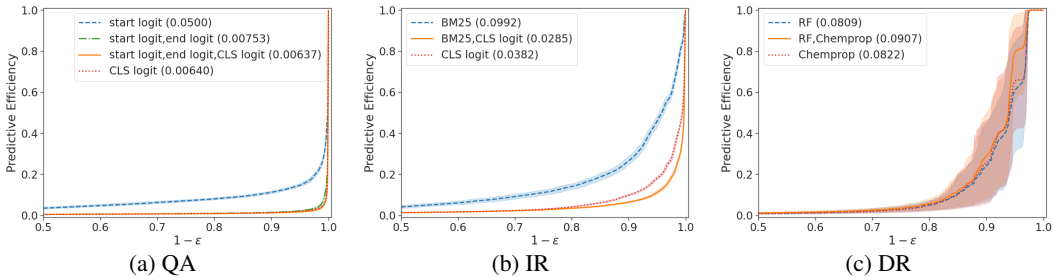


Figure 4: *How does cascading multiple nonconformity measures (§5.2) affect the predictive efficiency?* We observe that the first level typically greatly reduces the label space, while the subsequent levels then typically substantially improve the efficiency (QA, IR). In the DR task we observe a negative result, where the small sample size (the n in $\mathcal{C}_{n,\epsilon}$) causes the MHT-corrected CP to be too conservative. Surprisingly, on the test data, the cheaper RF measure on its own actually outperforms chemprop.

Non-conformal methods. For completeness, we next analyze how the performance of our conformal predictors compares to other non-conformal methods. We use two common heuristics for producing set-valued predictions—namely, taking the top- k predictions and taking all predictions for which the model’s score (e.g., the model logit or probability for $y|x$) exceeds a threshold τ , where we tune k and τ on the calibration set to get the desired accuracy (of $1 - \epsilon$). Even against the best baselines (that do not amortize cost or guarantee coverage), our method achieves better or comparable predictive efficiency on average. QA and IR do relatively better against the baselines than DR, however, as once again, DR is hampered by the small calibration set size. Appendix B.2 contains full results.

Future work. While our results show improvements in key areas, several challenges remain. Dealing with small sample sizes (which is often the case when the ratio of *positive* examples is low, as in DR) is one. Applying alternative, more data-efficient methods in-between *full* and *split* CP [4; 58, *inter alia*] could prove useful. The choice of cascaded nonconformity measures can also be optimized. The predictive efficiency is best when the measures are complementary; explicitly training for this could yield further improvements. Finally, the equivalence relations we consider are still fairly restrictive—they can be further relaxed in return for even larger efficiency gains.

8 Conclusion

Conformal prediction can afford remarkable theoretical performance guarantees to important applications for which high accuracy and precise confidence estimates are key. Naively applying CP, however, could be inefficient in practice. This is especially true in realistic domains in which the correct answers are not clearly delineated, and in which the computational cost of discriminating between options starts to become a limiting factor. In this paper, we proposed two simple extensions that provide two more pieces of the puzzle. Our results show that (1) calibrating for equivalent correctness consistently improves empirical predictive efficiency, and (2) conformal prediction cascades yield better computational efficiency—and thereby admit the use of more powerful classifiers.

Broader Impact

This work aims to improve two important aspects of conformal prediction for classification, namely, *predictive* and *computational* efficiency. In doing so, this work brings us closer to achieving practically usable classifiers with strong performance guarantees—a quality that is critical to many important applications. For example, in this work we applied our methods to information retrieval for fact verification, question answering, and computational chemistry for drug discovery (in-silico screening tools). We acknowledge that companies for which these types of tasks are particularly important—e.g., pharmaceutical companies in terms of the drug discovery setting—could stand to asymmetrically gain from a successful implementation of our work, but not unfairly so. The primary factors contributing to a failed system are the same for all standard conformal predictions, namely: (1) violations of the exchangeability assumption (resulting in invalid CPs), or (2) low statistical power in the nonformity measure (resulting in low predictive efficiency). The consequence of a failed system is primarily decreased utility as a precise prediction service, and ultimately, its use would simply be discontinued.

Acknowledgements

We thank Ben Fisch for helpful comments and discussion on this work, and thank Kyle Swanson for help in running the chemprop models. We also thank the MIT NLP group for valuable feedback. AF is supported in part by the National Science Foundation Graduate Research Fellowship under Grant #1122374. Any opinion, findings, conclusions, or recommendations expressed in this material are those of the authors and do not necessarily reflect the views of the the NSF or the U.S. Government.

References

- [1] Dario Amodei, Chris Olah, Jacob Steinhardt, Paul Christiano, John Schulman, and Dan Mané. Concrete problems in ai safety. *arXiv preprint arXiv:1606.06565*, 2016.
- [2] Arsenii Ashukha, Alexander Lyzhov, Dmitry Molchanov, and Dmitry Vetrov. Pitfalls of in-domain uncertainty estimation and ensembling in deep learning. In *International Conference on Learning Representations (ICLR)*, 2020.
- [3] Vineeth N. Balasubramanian, Shayok Chakraborty, and Sethuraman Panchanathan. Conformal predictions for information fusion. *Annals of Mathematics and Artificial Intelligence*, 74(1):45–65, 2015.
- [4] Rina Foygel Barber, Emmanuel J. Candes, Aaditya Ramdas, and Ryan J. Tibshirani. Predictive inference with the jackknife+. *arXiv preprint: arXiv 1905.02928*, 2019.
- [5] Wei Bi and James Kwok. Efficient multi-label classification with many labels. In *International Conference on Machine Learning (ICML)*, 2013.
- [6] Evgeny Burnaev and Vladimir Vovk. Efficiency of conformalized ridge regression. In *Conference on Learning Theory (COLT)*, 2014.
- [7] Maxime Cauchois, Suyash Gupta, and John Duchi. Knowing what you know: valid confidence sets in multiclass and multilabel prediction. *arXiv preprint: arXiv 2004.10181*, 2020.
- [8] Eugene Charniak, Mark Johnson, Micha Elsner, Joseph Austerweil, David Ellis, Isaac Haxton, Catherine Hill, R. Shrivaths, Jeremy Moore, Michael Pozar, and Theresa Vu. Multilevel coarse-to-fine PCFG parsing. In *Annual Conference of the North American Chapter of the Association for Computational Linguistics: Human Language Technologies (NAACL-HLT)*, 2006.
- [9] Danqi Chen, Adam Fisch, Jason Weston, and Antoine Bordes. Reading Wikipedia to answer open-domain questions. In *Annual Meeting of the Association for Computational Linguistics (ACL)*, 2017.
- [10] Wenyu Chen, Zhaokai Wang, Wooseok Ha, and Rina Foygel Barber. Trimmed conformal prediction for high-dimensional models. *arXiv preprint: arXiv 1611.09933*, 2016.
- [11] Wenyu Chen, Kelli-Jean Chun, and Rina Foygel Barber. Discretized conformal prediction for efficient distribution-free inference. *Stat*, 7(1):e173, 2018.

- [12] Giovanni Cherubin. Majority vote ensembles of conformal predictors. *Machine Learning*, 108(3):475–488, 2019.
- [13] Jay DeYoung, Sarthak Jain, Nazneen Fatema Rajani, Eric Lehman, Caiming Xiong, Richard Socher, and Byron C. Wallace. Eraser: A benchmark to evaluate rationalized nlp models. In *Annual Meeting of the Association for Computational Linguistics (ACL)*, 2020.
- [14] Ran El-Yaniv and Yair Wiener. On the foundations of noise-free selective classification. *Journal of Machine Learning Research (JMLR)*, 11(53):1605–1641, 2010.
- [15] Alessio Farcomeni. A review of modern multiple hypothesis testing, with particular attention to the false discovery proportion. *Statistical methods in medical research*, 17:347–88, 09 2007.
- [16] David Ferrucci, Eric Brown, Jennifer Chu-Carroll, James Fan, David Gondek, Aditya A. Kalyanpur, Adam Lally, J. William Murdock, Eric Nyberg, John Prager, Nico Schlaefer, and Chris Welty. Building watson: An overview of the deepqa project. *AI Magazine*, 31(3):59–79, Jul. 2010.
- [17] Francois Fleuret and Donald Geman. Coarse-to-fine face detection. *International Journal of Computer Vision*, 41(1–2):85–107, 2001.
- [18] Yarin Gal and Zoubin Ghahramani. Dropout as a bayesian approximation: Representing model uncertainty in deep learning. In *International Conference on Machine Learning (ICML)*, 2016.
- [19] Alexander Gammerman and Vladimir Vovk. Hedging Predictions in Machine Learning: The Second Computer Journal Lecture . *The Computer Journal*, 50(2):151–163, Feb. 2007.
- [20] Yonatan Geifman and Ran El-Yaniv. Selective classification for deep neural networks. In *Advances in Neural Information Processing Systems (NeurIPS)*, pages 4878–4887. 2017.
- [21] Chuan Guo, Geoff Pleiss, Yu Sun, and Kilian Q. Weinberger. On calibration of modern neural networks. In *International Conference on Machine Learning (ICML)*, 2017.
- [22] Lior Hirschfeld, Kyle Swanson, Kevin Yang, Regina Barzilay, and Connor W. Coley. Uncertainty quantification using neural networks for molecular property prediction. *arXiv preprint: arXiv 2005.10036*, 2020.
- [23] Robert A. Jacobs, Michael I. Jordan, Steven J. Nowlan, and Geoffrey E. Hinton. Adaptive mixtures of local experts. *Neural Computation*, 3(1):79–87, March 1991.
- [24] Heinrich Jiang, Been Kim, Melody Guan, and Maya Gupta. To trust or not to trust a classifier. In *Advances in Neural Information Processing Systems (NeurIPS)*, pages 5541–5552. 2018.
- [25] Xiaoqian Jiang, Melanie Osl, Jihoon Kim, and Lucila Ohno-Machado. Calibrating predictive model estimates to support personalized medicine. *Journal of the American Medical Informatics Association*, 19(2):263–274, Mar-Apr 2012.
- [26] Armand Joulin, Edouard Grave, Piotr Bojanowski, and Tomas Mikolov. Bag of tricks for efficient text classification. In *Conference of the European Chapter of the Association for Computational Linguistics (EACL)*, 2017.
- [27] Daniel Jurafsky and James H. Martin. *Speech and Language Processing: An Introduction to Natural Language Processing, Computational Linguistics, and Speech Recognition*. Prentice Hall PTR, USA, 1st edition, 2000. ISBN 0130950696.
- [28] Balaji Lakshminarayanan, Alexander Pritzel, and Charles Blundell. Simple and scalable predictive uncertainty estimation using deep ensembles. In *Advances in Neural Information Processing Systems*, pages 6402–6413. 2017.
- [29] Zhenzhong Lan, Mingda Chen, Sebastian Goodman, Kevin Gimpel, Piyush Sharma, and Radu Soricut. Albert: A lite bert for self-supervised learning of language representations. In *International Conference on Learning Representations (ICLR)*, 2020.
- [30] Kenton Lee, Tom Kwiatkowski, Ankur P. Parikh, and Dipanjan Das. Learning recurrent span representations for extractive question answering. *arXiv preprint: arXiv 1611.01436*, 2016.

- [31] Kimin Lee, Honglak Lee, Kibok Lee, and Jinwoo Shin. Training confidence-calibrated classifiers for detecting out-of-distribution samples. In *International Conference on Learning Representations (ICLR)*, 2018.
- [32] Jing Lei, Max G’Sell, Alessandro Rinaldo, Ryan J. Tibshirani, and Larry Wasserman. Distribution-free predictive inference for regression. *Journal of the American Statistical Association*, 113(523):1094–1111, 2018.
- [33] Haoxiang Li, Zhe Lin, Xiaohui Shen, Jonathan Brandt, and Gang Hua. A convolutional neural network cascade for face detection. In *Conference on Computer Vision and Pattern Recognition (CVPR)*, June 2015.
- [34] Henrik Linusson, Ulf Norinder, Henrik Boström, Ulf Johansson, and Tuve Löfström. On the calibration of aggregated conformal predictors. In *Proceedings of the Sixth Workshop on Conformal and Probabilistic Prediction and Applications*, 2017.
- [35] Wei Liu. Multiple tests of a non-hierarchical finite family of hypotheses. *Journal of the Royal Statistical Society. Series B (Methodological)*, 58(2):455–461, 1996.
- [36] Frederic Morin and Yoshua Bengio. Hierarchical probabilistic neural network language model. In *International Conference on Artificial Intelligence and Statistics (AISTATS)*, 2005.
- [37] Alexandru Niculescu-Mizil and Rich Caruana. Predicting good probabilities with supervised learning. In *International Conference on Machine Learning (ICML)*, 2005.
- [38] Yixin Nie, Haonan Chen, and Mohit Bansal. Combining fact extraction and verification with neural semantic matching networks. In *AAAI Conference on Artificial Intelligence (AAAI)*, 2019.
- [39] Harris Papadopoulos. Inductive conformal prediction: Theory and application to neural networks. In *Tools in Artificial Intelligence*, chapter 18. IntechOpen, Rijeka, 2008.
- [40] F. Pedregosa, G. Varoquaux, A. Gramfort, V. Michel, B. Thirion, O. Grisel, M. Blondel, P. Prettenhofer, R. Weiss, V. Dubourg, J. Vanderplas, A. Passos, D. Cournapeau, M. Brucher, M. Perrot, and E. Duchesnay. Scikit-learn: Machine learning in Python. *Journal of Machine Learning Research (JMLR)*, 12:2825–2830, 2011.
- [41] Pranav Rajpurkar, Robin Jia, and Percy Liang. Know what you don’t know: Unanswerable questions for SQuAD. In *Annual Meeting of the Association for Computational Linguistics (ACL)*, 2018.
- [42] Radim Řehůřek and Petr Sojka. Software Framework for Topic Modelling with Large Corpora. In *LREC 2010 Workshop on New Challenges for NLP Frameworks*. ELRA, 2010.
- [43] David Rogers and Mathew Hahn. Extended-connectivity fingerprints. *Journal of chemical information and modeling*, 50:742–54, 05 2010.
- [44] Yaniv Romano, Evan Patterson, and Emmanuel Candès. Conformalized quantile regression. In *Advances in Neural Information Processing Systems (NeurIPS)*. 2019.
- [45] Yaniv Romano, Rina Foygel Barber, Chiara Sabatti, and Emmanuel Candès. With malice toward none: Assessing uncertainty via equalized coverage. *Harvard Data Science Review*, 4 2020.
- [46] Alexander Rush and Slav Petrov. Vine pruning for efficient multi-pass dependency parsing. In *Conference of the North American Chapter of the Association for Computational Linguistics: Human Language Technologies (NAACL-HLT)*, 2012.
- [47] Einar Andreas Rødland. Simes’ procedure is ‘valid on average’. *Biometrika*, 93(3):742–746, 2006.
- [48] Benjamin Sapp, Alexander Toshev, and Ben Taskar. Cascaded models for articulated pose estimation. In *European Conference on Computer Vision (ECCV)*, 2010.

- [49] Sanat K. Sarkar and Chung-Kuei Chang. The simes method for multiple hypothesis testing with positively dependent test statistics. *Journal of the American Statistical Association*, 92(440):1601–1608, 1997.
- [50] Tal Schuster, Darsh Shah, Yun Jie Serene Yeo, Daniel Roberto Filizzola Ortiz, Enrico Santus, and Regina Barzilay. Towards debiasing fact verification models. In *Conference on Empirical Methods in Natural Language Processing and the International Joint Conference on Natural Language Processing (EMNLP-IJCNLP)*, 2019.
- [51] Glenn Shafer and Vladimir Vovk. A tutorial on conformal prediction. *Journal of Machine Learning Research (JMLR)*, 9:371–421, June 2008.
- [52] R. J. Simes. An improved Bonferroni procedure for multiple tests of significance. *Biometrika*, 73(3):751–754, 12 1986.
- [53] Jonathan Stokes, Kevin Yang, Kyle Swanson, Wengong Jin, Andres Cubillos-Ruiz, Nina Donghia, Craig MacNair, Shawn French, Lindsey Carfrae, Zohar Bloom-Ackerman, Victoria Tran, Anush Chiappino-Pepe, Ahmed Badran, Ian Andrews, Emma Chory, George Church, Eric Brown, Tommi Jaakkola, Regina Barzilay, and James Collins. A deep learning approach to antibiotic discovery. *Cell*, 180:688–702.e13, 02 2020.
- [54] James Thorne, Andreas Vlachos, Christos Christodoulopoulos, and Arpit Mittal. FEVER: a large-scale dataset for fact extraction and VERification. In *Conference of the North American Chapter of the Association for Computational Linguistics: Human Language Technologies (NAACL-HLT)*, 2018.
- [55] Ryan J Tibshirani, Rina Foygel Barber, Emmanuel Candes, and Aaditya Ramdas. Conformal prediction under covariate shift. In *Advances in Neural Information Processing Systems (NeurIPS)*. 2019.
- [56] Paolo Tocacceli and Alexander Gammerman. Combination of conformal predictors for classification. In *Sixth Workshop on Conformal and Probabilistic Prediction and Applications*, 2017.
- [57] Paolo Tocacceli and Alexander Gammerman. Combination of inductive mondrian conformal predictors. *Machine Learning*, 108(3):489–510, 2019.
- [58] Vladimir Vovk. Cross-conformal predictors. *Annals of Mathematics and Artificial Intelligence*, 74(1):9–28, 2015.
- [59] Vladimir Vovk, Alex Gammerman, and Glenn Shafer. *Algorithmic Learning in a Random World*. Springer-Verlag, Berlin, Heidelberg, 2005.
- [60] Vladimir Vovk, Ilia Nouretdinov, and Alex Gammerman. On-line predictive linear regression. *Annals of Statistics*, 37(3):1566–1590, 06 2009. doi: 10.1214/08-AOS622.
- [61] Vladimir Vovk, Valentina Fedorova, Ilia Nouretdinov, and Alexander Gammerman. Criteria of efficiency for conformal prediction. In *International Symposium on Conformal and Probabilistic Prediction with Applications - Volume 9653*, 2016.
- [62] Vladimir Vovk, Ivan Petej, Ilia Nouretdinov, Valery Manokhin, and Alexander Gammerman. Computationally efficient versions of conformal predictive distributions. *Neurocomputing*, 397: 292 – 308, 2020.
- [63] David Weiss and Benjamin Taskar. Structured prediction cascades. In *International Conference on Artificial Intelligence and Statistics (AISTATS)*, 2010.
- [64] Thomas Wolf, Lysandre Debut, Victor Sanh, Julien Chaumond, Clement Delangue, Anthony Moi, Pierric Cistac, Tim Rault, R’emi Louf, Morgan Funtowicz, and Jamie Brew. Huggingface’s transformers: State-of-the-art natural language processing. *arXiv preprint: arXiv 1910.03771*, 2019.
- [65] Zhenqin Wu, Bharath Ramsundar, Evan N. Feinberg, Joseph Gomes, Caleb Geniesse, Aneesh S. Pappu, Karl Leswing, and Vijay Pande. Moleculenet: a benchmark for molecular machine learning. *Chem. Sci.*, 9:513–530, 2018.

- [66] Kevin Yang, Kyle Swanson, Wengong Jin, Connor Coley, Philipp Eiden, Hua Gao, Angel Guzman-Perez, Timothy Hopper, Brian Kelley, Miriam Mathea, Andrew Palmer, Volker Settels, Tommi Jaakkola, Klavs Jensen, and Regina Barzilay. Analyzing learned molecular representations for property prediction. *Journal of Chemical Information and Modeling*, 59(8):3370–3388, 2019.

Appendix

A Proofs

A.1 Proof of Lemma 1

Proof. This is a well-known result; we prove it here for completeness (see also [55; 59] for a similar proof). It is straightforward to show that for $P = \text{pvalue}(V_{n+1}, V_{1:n})$

$$P \leq \epsilon \iff V_{n+1} \text{ is ranked among the } \lfloor \epsilon \cdot (n+1) \rfloor \text{ largest of } V_1, \dots, V_{n+1}.$$

According to our exchangeability assumption over the $n+1$ variables, the right hand side event occurs with at most probability $\lfloor \epsilon \cdot (n+1) \rfloor / (n+1) \leq \epsilon$. \square

A.2 Proof of Theorem 1

Proof. Once again, this is a well-known result; we prove it here for completeness (see also [55; 59] for a similar proof). Since the non-conformity scores $V_i^{(x_i, y_i)}$ are constructed symmetrically, then (simplifying notation by denoting $V_i^{(x_i, y_i)}$ as just V_i):

$$\begin{aligned} ((X_1, Y_1), \dots, (X_{n+1}, Y_{n+1})) &\stackrel{d}{=} ((X_{\sigma(1)}, Y_{\sigma(1)}), \dots, (X_{\sigma(n+1)}, Y_{\sigma(n+1)})) \\ \iff (V_1, \dots, V_{n+1}) &\stackrel{d}{=} (V_{\sigma(1)}, \dots, V_{\sigma(n+1)}) \end{aligned}$$

for all permutations $(\sigma(1), \dots, \sigma(n+1))$. Therefore, if $\{(X_i, Y_i)\}_{i=1}^{n+1}$ are exchangeable, then so too are their nonconformal scores $\{V_i\}_{i=1}^{n+1}$.

By the construction of $\mathcal{C}_{n,\epsilon}(X_{n+1})$, we have

$$Y_{n+1} \notin \mathcal{C}_{n,\epsilon}(X_{n+1}) \iff \text{pvalue}\left(V_{n+1}^{(x_{n+1}, y)}, V_{1:n}^{(x_{1:n}, y_{1:n})}\right) \leq \epsilon.$$

Then, using Lemma 1, $\mathbb{P}(Y_{n+1} \in \mathcal{C}_{n,\epsilon}(X_{n+1})) = 1 - \mathbb{P}(Y_{n+1} \notin \mathcal{C}_{n,\epsilon}(X_{n+1})) \geq 1 - \epsilon$. \square

A.3 Proof of Theorem 2

Proof. (1) First we prove that $\mathcal{C}_{n,\epsilon}^{\min}(X_{n+1})$ satisfies Eq. 5. We begin by establishing exchangeability of $M_i^{(x_i, y_i)}$, where $M_i^{(x_i, y_i)}$ is as defined in Eq. 6. We simplify notation once again by denoting $V_i^{(x_i, y_i)}$ as V_i , and $M_i^{(x_i, y_i)}$ as M_i . By the same argument as in the proof for Theorem 1, we have that the base $\{V_i\}_{i=1}^{n+1}$ are exchangeable. Since the equivalence class expansion and subsequent min operator are taken *point-wise* over the V_i , we retain symmetry, and therefore

$$(V_1, \dots, V_{n+1}) \stackrel{d}{=} (V_{\sigma(1)}, \dots, V_{\sigma(n+1)}) \implies (M_1, \dots, M_{n+1}) \stackrel{d}{=} (M_{\sigma(1)}, \dots, M_{\sigma(n+1)})$$

for all permutations $(\sigma(1), \dots, \sigma(n+1))$. Thus $\{M_i\}_{i=1}^{n+1}$ are also exchangeable.

Next, we want to prove that $\mathcal{C}_{n,\epsilon}^{\min}$ satisfies Eq. 5, i.e.:

$$\mathbb{P}\left(\left| [Y_{n+1}]_{R(X_{n+1})} \cap \mathcal{C}_{n,\epsilon}^{\min}(X_{n+1}) \right| \geq 1\right) \geq 1 - \epsilon.$$

To further simplify notation, we drop the dependence on X_{n+1} and (x_i, y_i) where obvious. Let $|[Y_{n+1}]_R| = k$, and rewrite $[Y_{n+1}]_R$ as $\{\tilde{Y}_1, \dots, \tilde{Y}_k\}$. Then:

$$\begin{aligned} \mathbb{P}\left(\left| [Y_{n+1}]_R \cap \mathcal{C}_{n,\epsilon}^{\min} \right| \geq 1\right) &= \mathbb{P}\left(\bigcup_{i=1}^k \tilde{Y}_i \in \mathcal{C}_{n,\epsilon}^{\min}\right) \\ &\geq \max\left\{\mathbb{P}\left(\tilde{Y}_1 \in \mathcal{C}_{n,\epsilon}^{\min}\right), \dots, \mathbb{P}\left(\tilde{Y}_k \in \mathcal{C}_{n,\epsilon}^{\min}\right)\right\} \\ &= \max\left\{\mathbb{P}\left(\text{pvalue}(V_{n+1}^{(\tilde{y}_1)}, M_{1:n}) > \epsilon\right), \dots, \mathbb{P}\left(\text{pvalue}(V_{n+1}^{(\tilde{y}_k)}, M_{1:n}) > \epsilon\right)\right\} \\ &\stackrel{(i)}{=} \mathbb{P}\left(\text{pvalue}(M_{n+1}, M_{1:n}) > \epsilon\right) \\ &\stackrel{(ii)}{\geq} 1 - \epsilon \end{aligned}$$

where (i) is by construction of M_{n+1} (assuming *w.l.o.g.* that it is unique in the case of the random tie-breaking in `pvalue`), and (ii) comes from applying Lemma 1 to the exchangeable $\{M_i\}_{i=1}^{n+1}$.

(2) We now prove the second part of Theorem 2: that $\mathbb{E} [|\mathcal{C}_{n,\epsilon}^{\min}(X_{n+1})|] \leq \mathbb{E} [|\mathcal{C}_{n,\epsilon}(X_{n+1})|]$. Again, to simplify notation, we drop the dependence on (x_i, y_i) where obvious.

Let $\mathbf{1}\{y_i \in \mathcal{C}_{n,\epsilon}\}$ be the indicator random variable that $y_i \in \mathcal{Y}$ is included in $\mathcal{C}_{n,\epsilon}$. Then:

$$\mathbb{E} [|\mathcal{C}_{n,\epsilon}|] = \mathbb{E} \left[\sum_{i=1}^{|\mathcal{Y}|} \mathbf{1}\{y_i \in \mathcal{C}_{n,\epsilon}\} \right] = \sum_{i=1}^{|\mathcal{Y}|} \mathbb{E} [\mathbf{1}\{y_i \in \mathcal{C}_{n,\epsilon}\}] = \sum_{i=1}^{|\mathcal{Y}|} \mathbb{P} (\text{pvalue}(V_{n+1}^{(y_i)}, V_{1:n}) > \epsilon).$$

By the same derivation we also have $\mathbb{E} [|\mathcal{C}_{n,\epsilon}^{\min}|] = \sum_{i=1}^{|\mathcal{Y}|} \mathbb{P} (\text{pvalue}(V_{n+1}^{(y_i)}, M_{1:n}) > \epsilon)$.

Since $M_i \leq V_i \forall i \in [1, n+1]$ by definition, we get that $V_{n+1} \leq M_i \Rightarrow V_{n+1} \leq V_i$, and it is the easy to see from the definition of the `pvalue` (see Eq. 2) that this leads to $\mathbb{P}(\text{pvalue}(V_{n+1}^{(y)}, M_{1:n}) > \epsilon) \leq \mathbb{P}(\text{pvalue}(V_{n+1}^{(y)}, V_{1:n}) > \epsilon), \forall y \in \mathcal{Y}$. Therefore, it follows that $\mathbb{E} [|\mathcal{C}_{n,\epsilon}^{\min}|] \leq \mathbb{E} [|\mathcal{C}_{n,\epsilon}|]$. \square

A.4 Proof of Theorem 3

Proof. We restate our assumption that \mathcal{M} is a valid multiple hypothesis testing correction procedure that properly controls the family-wise error rate,

$$\tilde{P}^{(x,y)} = \mathcal{M} \left(P_1^{(x,y)}, \dots, P_m^{(x,y)} \right) \text{ s.t. } \mathbb{P} \left(\tilde{P}^{(x,y)} \leq \epsilon \mid y \text{ is correct} \right) \leq \epsilon,$$

and that it is element-wise monotonic,

$$\left(P_1^{(x,y)}, \dots, P_m^{(x,y)} \right) \preccurlyeq \left(\hat{P}_1^{(x,y)}, \dots, \hat{P}_m^{(x,y)} \right) \implies \mathcal{M} \left(P_1^{(x,y)}, \dots, P_m^{(x,y)} \right) \leq \mathcal{M} \left(\hat{P}_1^{(x,y)}, \dots, \hat{P}_m^{(x,y)} \right),$$

where $P_i^{(x,y)}$ are p-values produced by different nonconformity measures for the same point (x, y) , and \preccurlyeq operates element-wise.

First we show that all $\mathcal{C}_{n,\epsilon}^m$ constructed via Eq. 11 satisfies Eq. 1 when all p-values are known and no pruning has been done. \mathcal{M} operates element-wise over examples, therefore exchangeability is conserved and all basic individual p-value computations from nonconformity scores are valid as before. Then, by the construction of $\mathcal{C}_{n,\epsilon}^m(X_{n+1})$, we have

$$Y_{n+1} \notin \mathcal{C}_{n,\epsilon}(X_{n+1}) \iff \tilde{P}^{(x_{n+1}, y_{n+1})} \leq \epsilon,$$

and therefore,

$$\begin{aligned} \mathbb{P} (Y_{n+1} \in \mathcal{C}_{n,\epsilon}^m(X_{n+1})) &= 1 - \mathbb{P} (Y_{n+1} \notin \mathcal{C}_{n,\epsilon}^m(X_{n+1})) \\ &= 1 - \mathbb{P} \left(\tilde{P}^{(x_{n+1}, y_{n+1})} \leq \epsilon \right) \\ &\geq 1 - \epsilon \end{aligned}$$

where the final inequality comes from the first assumption on \mathcal{M} .

Next, we want to prove that early pruning does not remove any candidates y that would *not* be removed from $\mathcal{C}_{n,\epsilon}^m$. When all p-values after step j are not yet known, we set $P_{k>j}^{x_{n+1}, y}$ to 1. Using the element-wise monotonicity of \mathcal{M} , we have:

$$\mathcal{M} \left(P_1^{(x_{n+1}, y)}, \dots, P_j^{(x_{n+1}, y)}, 1, \dots, 1 \right) \geq \mathcal{M} \left(P_1^{(x_{n+1}, y)}, \dots, \bar{P}_m^{(x_{n+1}, y)} \right)$$

where \bar{P}_k represents the not-yet-realized value for $P_{k>j}$. Therefore,

$$\left\{ y \in \mathcal{Y}: \tilde{P}_j^{(x_{n+1}, y)} > \epsilon \right\} \supseteq \left\{ y \in \mathcal{Y}: \tilde{P}_m^{(x_{n+1}, y)} > \epsilon \right\},$$

matching Eq. 8, and yielding $y \in \mathcal{C}_{n,\epsilon}^m(X_{n+1}) \Rightarrow y \in \mathcal{C}_{n,\epsilon}^j(X_{n+1}), \forall y \in \mathcal{Y}$. We finish by using the earlier result for $\mathcal{C}_{n,\epsilon}^m(X_{n+1})$ to get:

$$\mathbb{P} (Y_{n+1} \in \mathcal{C}_{n,\epsilon}^j(X_{n+1})) \geq \mathbb{P} (Y_{n+1} \in \mathcal{C}_{n,\epsilon}^m(X_{n+1})) \geq 1 - \epsilon, \quad \forall j \in [1, m].$$

\square

B Additional experimental results

We provide additional experimental results for the tasks described in §6. In B.1 we give (unnormalized) results for specific significance levels, ϵ . In B.2 we compare our method to non-conformal methods at fixed efficiency levels, as described in §7.

B.1 Results per significance level ϵ

Section 7 focuses on evaluating normalized predictive and computational efficiencies across all ϵ (i.e., by computing the AUC). Table 1 provides absolute numerical results for specific significance levels. The numbers confirm the trends in Figure 2: *min* calibration results in smaller prediction sets, especially at small values of ϵ . For example, on the QA task, *min* calibration yields prediction sets nearly $3\times$ smaller on average for $\epsilon = 0.01$. The cascade typically matches or improves the predictive efficiency of the single CP, with a reduced computational cost. Note that when the calibration set is small, conformal prediction is ineffective for small ϵ . For example, with only $n \approx 30$ screens for calibration, the DR task is forced to output the full \mathcal{Y} (100 molecules) for all $\epsilon < 0.03$, as it is impossible to obtain a p-value smaller than $1/(n+1)$. As ϵ increases, the efficiency for DR rapidly improves (dramatically so, relative to the standard CP). The IR cascade is narrowly empirically under-calibrated at some values of epsilon; all other results prove empirically valid.

Table 1: CP results on the test set for different tolerance levels ϵ . Each line shows the empirical success rate (Succ.) and the size of the prediction set ($|\mathcal{C}_{n,\epsilon}|$) for our two extensions compared to regular CP per target success rate ($1 - \epsilon$). The amortized computation cost by the cascade, a consequence of the early pruning, is also given.

Task	$1 - \epsilon$	CP		<i>min</i> CP		Cascaded <i>min</i> CP		
		Succ.	$ \mathcal{C}_{n,\epsilon} $	Succ.	$ \mathcal{C}_{n,\epsilon}^{\min} $	Succ.	$ \mathcal{C}_{n,\epsilon}^{\min} $	Amortized cost
QA	0.99	1.00	17.69	0.99	6.68	0.99	6.31	0.50
	0.95	0.98	5.14	0.95	3.14	0.96	2.45	0.42
	0.90	0.95	3.09	0.90	1.98	0.92	1.76	0.40
	0.80	0.86	1.66	0.80	1.31	0.83	1.24	0.38
IR	0.99	0.99	19.08	0.99	17.87	0.99	12.06	0.98
	0.95	0.96	8.58	0.95	7.49	0.94	4.61	0.89
	0.90	0.92	5.02	0.90	4.08	0.89	2.64	0.81
	0.80	0.84	2.40	0.80	1.72	0.79	1.40	0.72
DR	0.99	1.00	100.00	1.00	100.00	1.00	100.00	1.00
	0.95	0.99	93.50	0.97	65.16	0.98	79.00	1.00
	0.90	0.98	77.34	0.91	25.14	0.92	28.50	0.80
	0.80	0.96	50.12	0.80	4.69	0.82	5.57	0.62

B.2 Non-conformal methods

In addition to evaluating our improvements over regular conformal prediction, we compare our conformal method to other common heuristics for making set-valued predictions. Specifically, we consider baseline methods that given some scoring function $\text{score}(x, y)$ and threshold τ , define the output set of predictions \mathcal{B} at $x \in \mathcal{X}$ as

$$\mathcal{B}(x, \tau) := \{y \in \mathcal{Y}: \text{score}(x, y) \geq \tau\}, \quad (12)$$

where τ is then tuned on the calibration set to find the largest threshold that still gives at least the desired empirical equivalent success rate:

$$\tau_\epsilon^* := \sup \left\{ \tau: \frac{1}{n} \sum_{i=1}^n \mathbf{1}\{|[y_i]_{R(x_i)} \cap \mathcal{B}(x_i, \tau)| \geq 1\} \geq 1 - \epsilon \right\}. \quad (13)$$

The prediction for the test point x_{n+1} is then $\mathcal{B}(x_{n+1}, \tau_\epsilon^*)$. We consider two variants: (1) fixed top- k , where $\text{score} := -\text{rank}(\text{metric}(x, y))$ according to some metric, and (2) raw thresholding, where $\text{score} := \text{metric}(x, y)$, i.e., some raw, unnormalized metric. Top- k is simple and relatively robust to the variance of the metric used, but as it doesn't depend on x , it also means that both easy examples and hard examples are treated the same (giving prediction sets that are too large in the former, and too

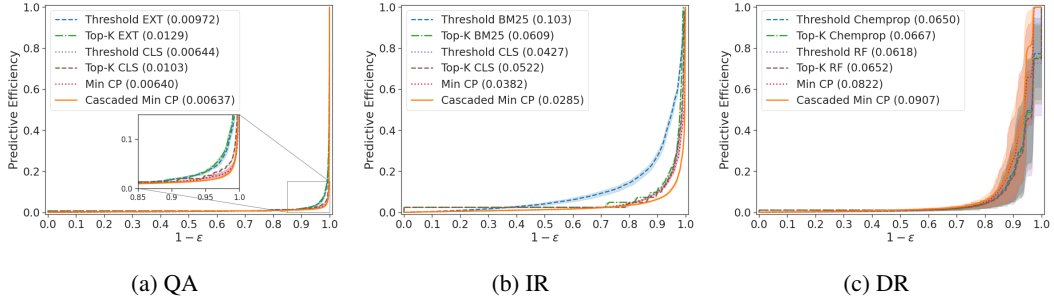


Figure 5: *How does our conformal method compare to non-conformal baselines?* We show predictive efficiency and equivalent success rates across various target accuracies (values of $1 - \epsilon$). On QA and IR the conformal methods match or exceed even the best baselines (that use the most expensive measures)—while maintaining a marginal coverage guarantees for finite-sample exchangeable data, which the baselines do not provide. As in §7, the DR task exhibits room for improvement, as it slightly under-performs the baselines on efficiency. Specific values of $1 - \epsilon$ are compared in Table 2.

small in the latter). Raw metric thresholding, on the other hand, gives dynamically-sized prediction sets, but is more sensitive to variance. We emphasize that these baselines do not provide theoretical coverage guarantees for potentially non-i.i.d. finite samples. They can also be quite computationally expensive (depending on `metric`). Nevertheless, it is useful to empirically compare these methods against our CP method for reference.

Figure 5 and Table 2 present the results. Figure 5 computes the AUC for predictive efficiency over the full range of $\epsilon \in (0, 1)$, while Table 2 lists absolute efficiencies and success rates at specific target values of $1 - \epsilon$. On both QA and IR, our *min*-Cascaded CP matches or outperforms all baselines (in addition to amortizing cost, see Table 1). For example, at a success rate of 99%, the *min*-Cascaded CP for IR attains nearly 2× better efficiency than the next best baseline (thresholded CLS). Note that one advantage of our cascade is that it allows us to easily combine different model types—i.e., the BM25 retriever with the neural CLS model—which is otherwise non-trivial. On DR, as before, CP performance suffers at low values of ϵ (trailing the baselines)—but starts to catch up with comparable efficiencies at higher values of ϵ .

Table 2: Non-CP baseline results on the test set for different target success rates $1 - \epsilon$. We compare the predictive efficiencies of our cascaded conformal method ($|\mathcal{C}_{n,\epsilon}^{\min}|$) to the predictive efficiencies of the baseline methods ($|\mathcal{B}|$). For the baselines, we combine different choices of `metric` (e.g., EXT) with different choices of `score` (e.g., top- k).

Task	$1 - \epsilon$	Threshold				Top- k				Cascaded <i>min</i> CP	
		EXT		CLS		EXT		CLS		Succ.	$ \mathcal{C}_{n,\epsilon}^{\min} $
		Succ.	$ \mathcal{B} $	Succ.	$ \mathcal{B} $	Succ.	$ \mathcal{B} $	Succ.	$ \mathcal{B} $	Succ.	$ \mathcal{C}_{n,\epsilon}^{\min} $
QA	0.99	0.99	21.50	0.99	9.26	0.99	18.54	0.99	6.66	0.99	6.31
	0.95	0.96	5.10	0.96	3.90	0.95	5.06	0.95	3.16	0.96	2.45
	0.90	0.92	2.86	0.91	2.00	0.90	2.71	0.90	2.00	0.92	1.76
	0.80	0.84	1.42	0.91	2.00	0.80	1.39	0.81	1.33	0.83	1.24
IR	BM25		CLS		BM25		CLS		BM25 → CLS		
	0.99	0.99	38.92	0.99	24.01	0.99	34.34	0.99	21.76	0.99	12.06
	0.95	0.96	8.96	0.95	7.86	0.95	19.75	0.95	7.98	0.94	4.61
	0.90	0.90	4.30	0.91	3.84	0.90	11.28	0.90	4.31	0.89	2.64
DR	0.80	0.82	2.00	0.85	1.88	0.80	5.87	0.80	1.79	0.79	1.40
	RF		chemprop		RF		chemprop		RF → chemprop		
	0.99	0.98	74.84	0.98	75.49	0.98	72.72	0.98	77.30	1.00	100.00
	0.95	0.95	45.53	0.95	48.42	0.95	45.15	0.95	49.45	0.98	79.00
	0.90	0.90	16.97	0.90	18.27	0.89	17.30	0.90	19.00	0.92	28.50
	0.80	0.82	4.17	0.82	3.89	0.79	4.24	0.79	3.95	0.82	5.57

C Implementation details

Multiple labelled answers. When multiple answers are given (i.e., Y_{n+1} is a set) we take the equivalence class as the union of all the equivalence classes of each answer. For the standard conformal predictor, we calibrate on one of the answers at a time, chosen uniformly at random. Note that this is important to preserve equivalent sample sizes across \min -calibrated CP and standard CP.⁶

QA. We use the SQuAD 2.0 extractive question answering dataset [41]. It contains 130,319 questions from 442 articles for training, and a development set with 11,873 questions from 48 articles. The authors keep the original test set hidden; for ease of CP-specific evaluation we re-split the development set randomly by article. This results in 5,302 questions in our validation set, and 6,571 questions in our test set. The average length of a paragraph in the evaluation set is 127 words. Together with the “no answer” option, a question for a paragraph of that length will have 8,129 candidate answer spans. For the purposes of experimentation, we filter out questions for which the EXT model (described next) does not give the correct answer to within the top 150 predictions (so we can compute the full $0 - 1$ range of ϵ tractably). Note that this discards less than 0.5% of questions.

Our span extractor model (EXT) uses the HuggingFace [64] implementation of the ALBERT-base QA model [29]. The model predicts two scores for each token in the paragraph independently: (1) a answer “start span” score, and (1) a answer “end span” score. The scores are trained to maximize the likelihood of span $[i, j]$, where $p(\text{start} = i, \text{end} = j)$ is modelled as $p(\text{start} = i) \times p(\text{end} = j)$. During inference, the model computes all combined start and end position scores, and predicts the answer with the highest combined score. In our model we use the both the start and end position scores as two separate nonconformity measures.

Our answer classifier (CLS) is also built on top of ALBERT-base, and is similar to Lee et al. [30]. Instead of scoring start and end positions independently, we concatenate the corresponding hidden representations at tokens i (start) and j (end), and score them jointly using an MLP. We then train with a binary cross-entropy (BCE) over correct and incorrect answers. We limit the number of negative samples (incorrect answers) to the top 64 wrong predictions of the EXT model.

IR. We use the FEVER dataset for evidence retrieval and fact verification [54]. We focus on the retrieval part of this task (the retrieved evidence can then be used to verify the correctness of the claim automatically [38; 50], or manually by a user). We follow the dataset splits of the Eraser benchmark [13] that contain 97,957 claims for training, and 6,122 and 6,111 claims for validation and test, respectively. The evidence needs to be retrieved from a set of 40,133 unique sentences collected from 4,099 total Wikipedia articles.

Our BM25 retriever uses default BM25 configuration available in the Gensim library [42]. We perform simple pre-processing to the text, such as removing punctuation and adding word stems. We also add the article title to each sentence. Our neural classifier (CLS) is built on top of ALBERT-base and is trained with BCE on (claim, evidence) pairs. We collect 10 negative pairs for each positive one by randomly selecting sentences from the same article as the correct evidence. For short articles, we extend the negative sampling to include the top candidates as retrieved by the BM25 retriever.

DR. Following Wu et al. [65], we use the HIV dataset introduced by the Drug Therapeutics Program (DTP) AIDS Antiviral Screen.⁷ This dataset contains 41,127 compounds, from which 1,443 were found to have some degree of activity when tested for the ability to inhibit HIV replication. We follow the randomized train, validation, and test data splits released with the chemprop model [66]. These splits contain 147 positives and 3,966 negatives in the validation set, and 132 positives and 3,981 negatives in the test set. The rest of the 1,164 positives and 33,180 negatives are used for training the classifiers. To simulate multiple random trials, in each trial, we randomly split the positive compounds into “screening” groups that, together with randomly samples negative compounds, create a set of 100 candidates. The number of positive compounds in each screening is sampled from a zero-truncated Pois(3) distribution (where we prevent the number of positives from being 0).

Both our random forest (RF) and the Directed Message Passing Neural Network (which we refer to generally as chemprop) were implemented using the chemprop repository [66]. The RF model is based on the Scikit library [40] and uses the binary Morgan fingerprints [43] to predict if a given compound is positive or not. The RF model is fast to run during inference, even on a single CPU.

⁶Another possibility would be to calibrate on *all* the given answers, but we found this generally does worse.

⁷<https://wiki.nci.nih.gov/display/NCIDTPdata/AIDS+Antiviral+Screen+Data>

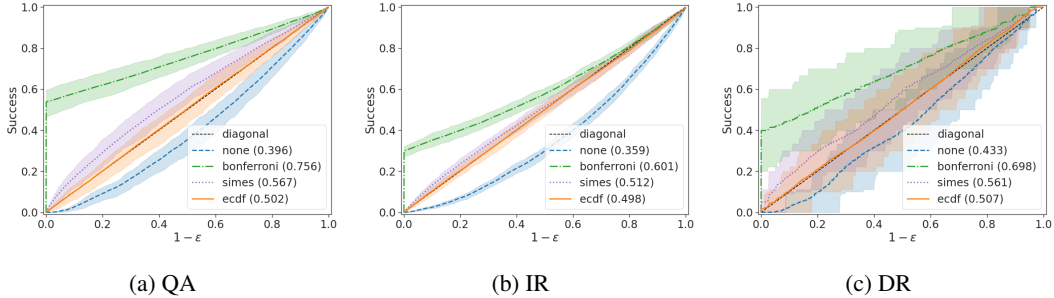


Figure 6: Success rate against tolerance thresholds for different methods for MHT correction (validation set). Not applying any correction leads to an invalid classifier (the success rate is below the diagonal). The Bonferroni method is conservative, leading to a valid classifier, but one with a higher success rate than necessary (a result of having excessively large $\mathcal{C}_{n,\epsilon}$). The Simes correction works for our tasks and provides a tighter bound. The ECDF correction is also well-calibrated in practice.

The `chemprop` model uses graph convolutions to learn a deep molecular representation. The final prediction of `chemprop` is based on an ensemble of 5 models, trained with different random seeds.

Table 3: Nonconformity measures used in our experiments.

Task	Metric	Description
QA	Start logit	$-1 \cdot$ logit of the answer’s first token using the EXT model.
	End logit	$-1 \cdot$ logit of the answer’s last token using the EXT model.
	CLS logit	$-1 \cdot$ logit of the joint answer pair using the CLS model.
IR	BM25	$-1 \cdot$ BM25 similarity score between query and candidate.
	CLS logit	$-1 \cdot$ logit of the claim-evidence pair using CLS.
DR	RF	$1 -$ score of the candidate using the Random Forest model.
	Chemprop	$1 -$ score of the candidate using the <code>chemprop</code> model.

D Multiple hypothesis testing

As we discuss in §5.2, naively combining multiple hypothesis tests will lead to an increased family-wise error rate (FWER). For a visual example, see the uncorrected cascaded CP (blue dashed line) in Figure 6. It demonstrates that combining nonconformal measures without using a MHT correction can result in success rates smaller than $1 - \epsilon$ (i.e., invalid coverage).

Several methods exist for correcting for MHT by bounding the FWER (with different assumptions on the dependencies between the hypothesis tests). We experiment with the Bonferroni, Simes, and ECDF procedures. For completeness, we briefly describe the three methods and the assumptions they rely on below (extensive additional details can be found in the literature). We also provide our validation results for the Bonferroni, Simes, and ECDF corrections.

D.1 Bonferroni Procedure

The Bonferroni correction is easy to apply and does not require any assumptions on the dependencies between the hypothesis tests used (e.g., independent, positively dependent, etc.). However, it is generally very conservative. The Bonferroni correction scales ϵ by a factor of $1/m$, and uses the union bound on the p-values (P_1, \dots, P_m) to get:

$$\mathbb{P}(Y_{n+1} \in \mathcal{C}_{n,\epsilon}^m(X_{n+1})) = \mathbb{P}\left(\bigcup_{i=1}^m P_i \leq \frac{\epsilon}{m}\right) \leq \sum_{i=1}^m \mathbb{P}\left(P_i \leq \frac{\epsilon}{m}\right) = \epsilon.$$

We achieve the same result by scaling each p-value by m , and take the final combined p-value to be the minimum of all the scaled p-values. It is easy to show that this correction is monotonic.

D.2 Simes Procedure

The Simes procedure [52] allows a stricter bound on the FWER when the measures are multivariate totally positive [49], which usually holds in practice [47]. We empirically found Simes to hold in all of our experiments. To apply the correction, we first sort the p-values in ascending order, and then perform an order-dependent correction where the bound becomes tighter as the p-value increases. Specifically, if $(P_{(1)}, \dots, P_{(m)})$ are the sorted p-values (P_1, \dots, P_m) in an m -level cascade, we modify the p-values to be $P_{(i)}^{\text{Sim}} = m \cdot \frac{P_{(i)}}{i}$. We take the final combined p-value to be the minimum of the corrected p-values. It is easy to show that this correction is monotonic.

D.3 ECDF Procedure

Toccaceli and Gammerman [57] proposed a simple calibration method based on the empirical CDF (see also [3]). Given a calibration set of n multivariate samples of dimension m , $\{(V_1^{(i)}, \dots, V_m^{(i)})\}_{i=1}^n$, we directly estimate the (right-tailed) CDF of the joint distribution:

$$\mathbb{P}(V_1 \geq v_1, \dots, V_m \geq v_m) \approx \frac{1}{n} \sum_{i=1}^n \mathbf{1} \left\{ V_1^{(i)} \geq v_1, \dots, V_m^{(i)} \geq v_m \right\}$$

Let $F_{V_1, \dots, V_m}(v_1, \dots, v_m) := \mathbb{P}(V_1 \geq v_1, \dots, V_m \geq v_m)$. In the univariate case ($m = 1$), the random variable $Y := F_{V_1, \dots, V_m}(V_1, \dots, V_m)$ follows the uniform distribution, but in the multivariate case ($m > 1$), it does not. In the multivariate case, we apply the correction again, this time on Y :

$$\mathbb{P}(Y \leq y) \approx \frac{1}{n} \sum_{i=1}^n \mathbf{1} \left\{ Y^{(i)} \leq y \right\}$$

It is easy to show that the random variable $X := F_Y(Y)$, where $F_Y(y) := \mathbb{P}(Y \leq y)$ like before, follows the uniform distribution. It is also easy to show that this correction is monotonic. This method can also be thought of as first computing a *combined* nonconformity measure using the CDF, and then computing a p-value for that derived metric (i.e., p-value of Y).

To be fully exchangeable and unbiased, the two calibration steps should either use disjoint calibration data or the CDF in the first part should be computed using the *full* CP method. This effect diminishes as n grows. In practice, if the dataset is large, we ignore this bias, and use the same calibration set for both the first and second ECDF computations with reasonable results. Otherwise, we use the full CP method (and include $\mathcal{S}(x_{n+1}, y)$ in the calibration step).

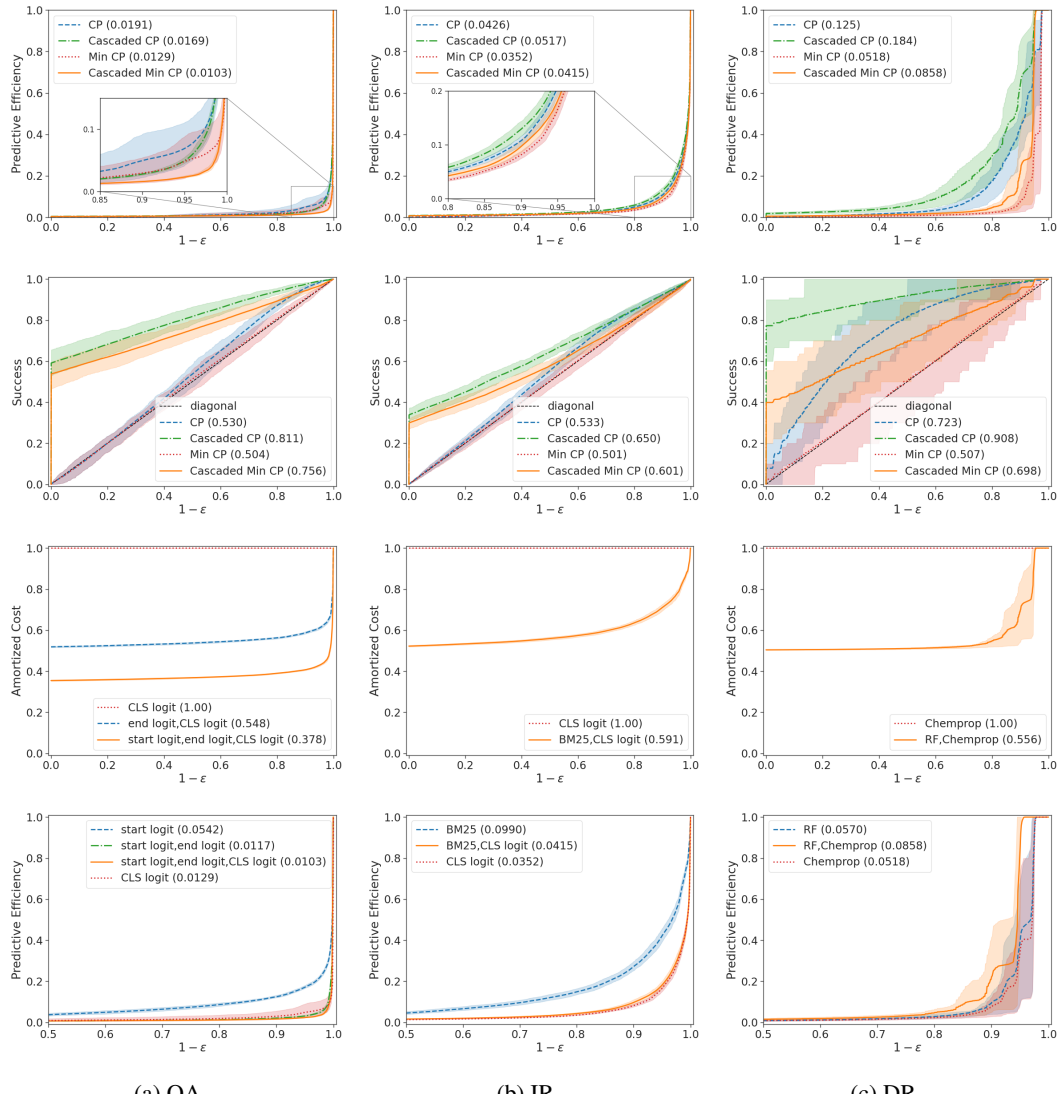


Figure 7: Validation results using the Bonferroni MHT correction.

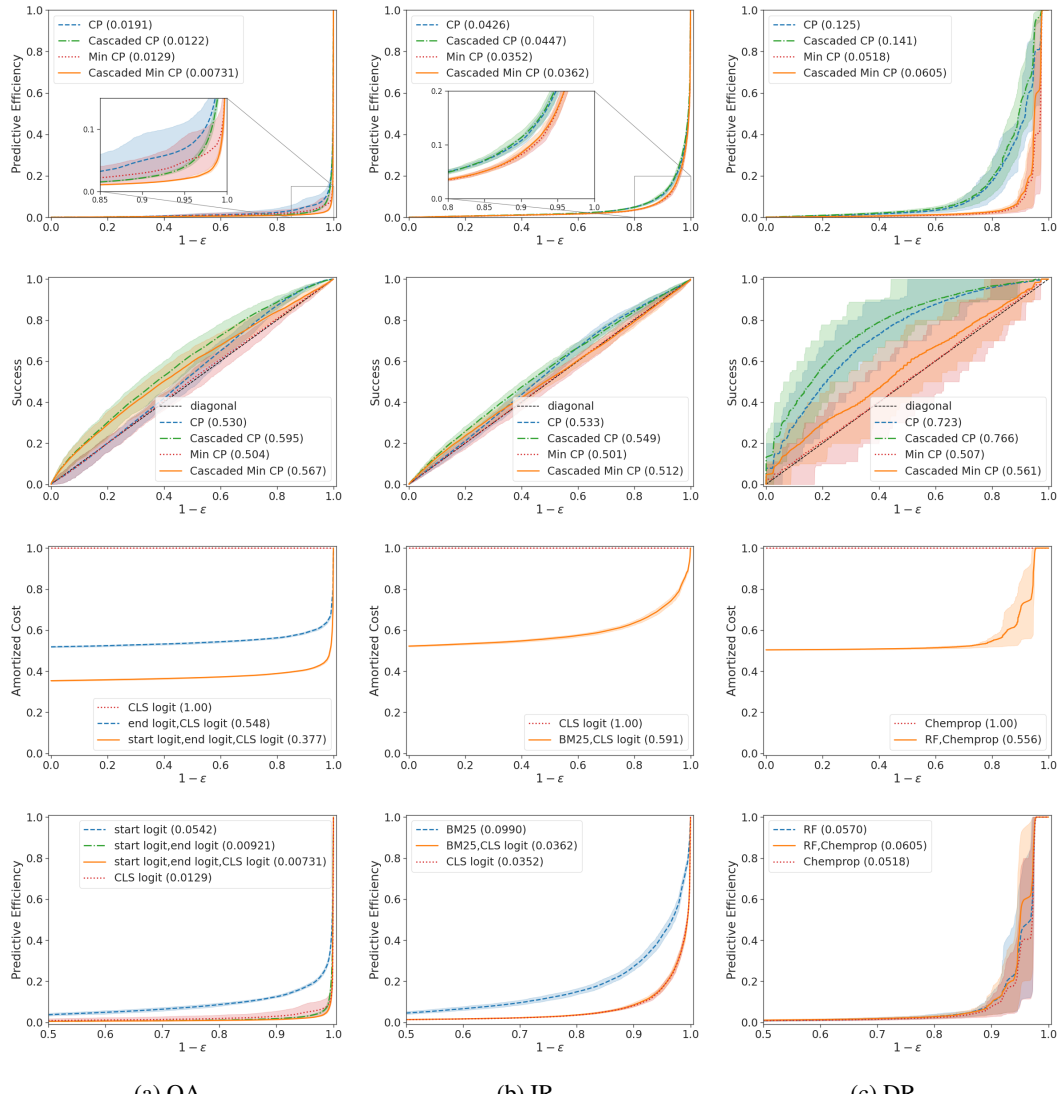


Figure 8: Validation results using the Simes MHT correction.

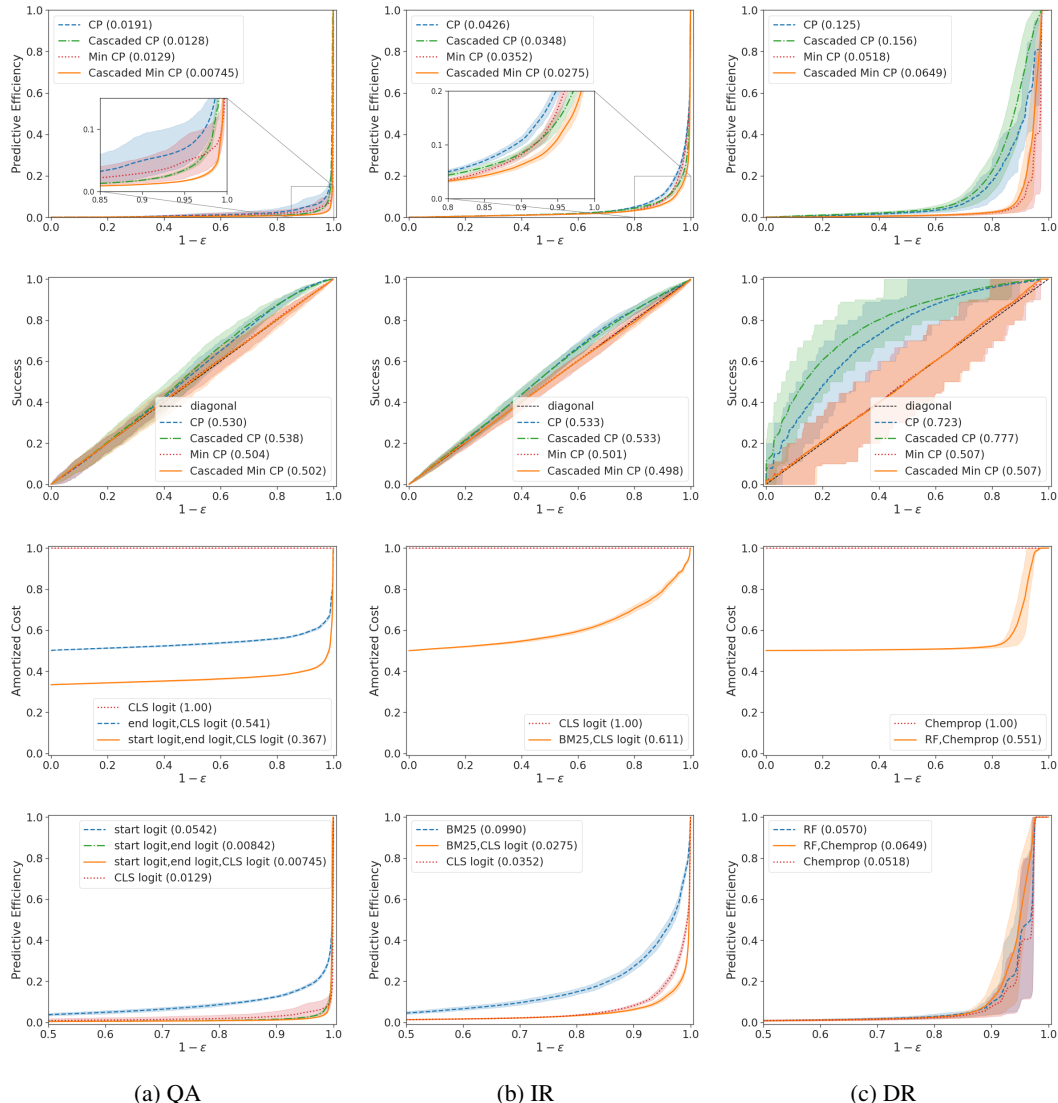


Figure 9: Validation results using the ECDF MHT correction.